(2+1') rotationally resolved resonance enhanced multiphoton ionization via the E 2∑+(4s,3d) and H 2∑+(3d,4s) Rydberg states of NO

H. Rudolph and V. McKoy

Citation: The Journal of Chemical Physics **93**, 7054 (1990); doi: 10.1063/1.459428
View online: http://dx.doi.org/10.1063/1.459428
View Table of Contents: http://scitation.aip.org/content/aip/journal/jcp/93/10?ver=pdfcov
Published by the AIP Publishing

(2+1′) rotationally resolved resonance enhanced multiphoton ionization via the $E^2\Sigma^+(4s,3d)$ and $H^2\Sigma^+(3d,4s)$ Rydberg states of NO

H. Rudolph and V. McKoy
Arthur Amos Noyes Laboratory of Chemical Physics, California Institute of Technology, Pasadena, California 91125

(Received 4 May 1990; accepted 23 July 1990)

The results of studies of ionic rotational branching ratios and photoelectron angular distributions resulting from (2 + 1′) resonance enhanced multiphoton ionization of NO via various high J ($\approx$21.5) rotational branches of the $E^2\Sigma^+(4s,3d)$ and $H^2\Sigma^+(3d,4s)$ Rydberg states are presented. The rotational branching ratios show the expected ΔN = even rotational propensity rule with very small ΔN = odd signals. The branching ratios for the $E^2\Sigma^+$ state are seen to be independent of photoelectron energy with the $\Delta N = +2$ signals strongest and no appreciable higher rotational transfer peaks ($|\Delta N| \geqslant 3$). The higher rotational transfer signal for ionization of the $H^2\Sigma^+$ state are also negligible but the rotational branching ratios are strongly energy dependent due to a Cooper minimum in the $l = 3$ partial wave of the $k\sigma$- and $k\pi$-continua at a photoelectron kinetic energy of 2.6 eV and 2.9 eV, respectively. This leads to a strong rotational selectivity that can be exploited to produce ions in a specific rotational level. These consequences of Cooper minima close to threshold are quite general and their influence on rotational distributions should be readily observable in other molecular systems. The photoelectron angular distributions via both states show a strong energy dependence with a rapid change in the angular distributions around the Cooper minimum associated with the $H^2\Sigma^+$ state.

I. INTRODUCTION

Resonance enhanced multiphoton ionization (REMPI) combined with high resolution photoelectron spectroscopy (PES) is proving to be a useful and sensitive probe of excited molecular states and their photoionization dynamics.[1-5] In several recent papers we have demonstrated how various aspects of the molecular photoionization dynamics influences the resulting photoelectron spectra and we have shown how these features can be used to probe the intermediate state's alignment, its character, and possible perturbations.[5-11] In previous rotationally resolved REMPI studies of NO we have found the rotational branching ratios and the rotationally resolved PES to be strongly dependent on the character and excitation scheme by which the intermediate state is accessed. For some Rydberg states, e.g., the $D^2\Sigma^+(3p\sigma)$ state of NO, the branching ratios display significant nonatomic character[7] and are quite energy dependent. On the other hand, they can be rather atomiclike and almost energy independent, as in the $A^2\Sigma^+(3s\sigma)$ state of NO.[3,4,7,9] In a recent paper we have similarly shown that a Cooper minimum in the photoionization spectra can have a profound effect on the resulting rotational branching ratios as the angular momentum composition of the transition moment changes character around the Cooper minimum.[11,12]

In this paper we present the results of studies of REMPI spectra for two higher $^2\Sigma^+$ Rydberg states of NO, the $E^2\Sigma^+(4s,3d)$ and $H^2\Sigma^+(3d,4s)$ states. These states have strong s and d character,[13-15] in contrast to the lower-lying $D^2\Sigma^+$ state which is almost 100% p-like.[5-7,15] This mixing of the $3d$ and $4s$ "states" leads to unusual quantum defects. With this composition of the resonant states ($l_0 = 0,2$) an atomic picture of photoionization out of these orbitals predicts strong transition moments to the odd partial wave components ($l = 1,3,...$) of the photoelectron continuum. The rotational selection rule,[7,16,17] $\Delta N + l$ = odd, where ΔN is the difference between the angular momentum of the final ionic state and the intermediate state (exclusive of spin), hence predicts rotational spectra dominated by a ΔN = even peaks ($\Delta N = 0, \pm 2, \pm 4,...$). In fact, our calculated branching ratios are, as expected, dominated by these even ΔN peaks. However, the branching ratios and photoelectron angular distributions for REMPI via the $H^2\Sigma^+$ state are strongly energy dependent due to a Cooper minimum close to threshold.[11] Around this Cooper minimum ions are produced in essentially a single rotational state, suggesting that this feature could be exploited for rotational selectivity in REMPI spectra. The rotational branching ratios and their photoelectron angular distributions are also seen to depend on the alignment of the intermediate state. Previous REMPI experiments via the E and the H state have been rotationally unresolved in the final ion state.[18,19] Preliminary data of Leahy *et al.*[20] for (2 + 1′) REMPI via the $E^2\Sigma^+$ state show encouraging agreement with the present results.

II. THEORY AND CALCULATIONAL DETAILS

The (2 + 1′) REMPI process is viewed as a two-photon excitation from an initially unaligned (all M_J levels equally populated) ground state ($X^2\Pi$) to an aligned intermediate state ($E^2\Sigma^+$ or $H^2\Sigma^+$), followed by ionization out of this state,[21]

 0021-9606/90/227054-12$03.00

$$\begin{aligned} &\mathrm{NO}\, X^2\Pi(v_0=0,J_0) \\ &\xrightarrow{2h\nu} \mathrm{NO}^*\, R^2\Sigma^+(v_i=0,J_i,N_i) \\ &\xrightarrow{h\nu} \mathrm{NO}^+\, X^1\Sigma^+(v_+=0,J_+=N_+)+e^-(\mathbf{k}), \end{aligned} \tag{1}$$

where $R^2\Sigma^+$ denotes an intermediate resonant $^2\Sigma^+$ Rydberg states. In the present study, both photons are linearly polarized along the same axis. In the absence of collisions and other M_J mixing interactions, each M_J level can be treated as an individual ionization channel. For the low laser intensities assumed here, the relative population of the M_J levels (ρ_{ii}) of the intermediate Rydberg state ($|i\rangle$) is well described by

$$\rho_{ii} \propto \begin{pmatrix} J_0 & 2 & J_i \\ M_i & 0 & -M_i \end{pmatrix}^2 B, \tag{2}$$

where B is the rotational line-strength,[22] and J_i and J_0 are defined in Eq. (1). The total photoionization signal is hence an incoherent sum over all M_J levels and rotational states accessed (see later). The probability $P(\theta,\phi)$ of photoelectron ejection in the direction (θ,ϕ) with respect to the laser polarization vector is given by

$$\begin{aligned} P(\theta,\phi) &= \sum_{\text{branches}} \sum_i \rho_{ii}\Gamma_i(J_i,N_i,N_+) \\ &= \sum_{L=0}^{L_{\max}/2} \beta_{2L} P_{2L}(\cos\theta), \end{aligned} \tag{3}$$

where $\Gamma_i(J_i,N_i,N_+)$ is the rotationally resolved ionization width. The photoelectron angular distributions can be expressed as a weighted sum over Legendre polynomials of even order, as seen in Eq. (3). Note that $L_{\max}$ is 6 for the present $(2+1')$ low intensity high-J experiments and can, in general, be determined for a particular REMPI process.[21]

We assume the $X^2\Pi$ ground state of NO to be intermediate between Hund's coupling case (a) and Hund's case (b), and the resonant $^2\Sigma^+$ and final $^1\Sigma^+$ states to be adequately described by Hund's case (b) coupling.[22,23] The E and $H^2\Sigma^+$ states are high-lying Rydberg states which may therefore be slightly rotationally decoupled from the nuclear rotation of the molecular core. They should therefore, in principle, be treated via an intermediate coupling scheme between Hund's cases (b) and (d). However the deviation from Hund's case (b) has previously been found to be minor[24] and is therefore neglected here. In the present frozen-core and orbital approximation,[21] the photoionization probability for a particular M_J level $\Gamma_i(M_J)$ is proportional to $\langle f|\mu|i\rangle^2$, the square of the one-electron matrix element between the final continuum orbital, $|f\rangle$, and the resonant Rydberg orbital, $|i\rangle$. For the REMPI process of Eq. (1) $\langle f|\mu|i\rangle$ can be written as[17]

$$\begin{aligned} \langle f|\mu|i\rangle = \sum_{N_t,\zeta} R(N_t,\zeta) \sum_{\mu} r_{fi}^{l\mu\mu}(-1)^{\mu} \\ \times \begin{pmatrix} N_+ & N_i & N_t \\ 0 & 0 & 0 \end{pmatrix} \begin{pmatrix} N_t & 1 & l \\ 0 & \mu & -\mu \end{pmatrix}, \end{aligned} \tag{4}$$

where $r_{fi}^{l\mu\mu}$ is a partial wave component of the bound-free matrix element and N_+ and N_i are the angular momenta of the ion and the resonant intermediate state (exclusive of spin), respectively. N_t is the angular momentum transfer, l is a partial wave of the photoelectron orbital, and μ its corresponding projection on the molecular axis. In the present case, for ionization out of a σ-orbital with linearly polarized light, $\mu = 0$ and ± 1 for ionization to the $k\sigma$ and $k\pi$- channels, respectively.[8] The $R(N_t,\zeta)$ term consists of various other 3-j symbols and phase factors, the detailed structure of which is of minor importance for the following discussion. These terms have, however, been included in the evaluation of the present results. Details are given in Ref. 17.

The partial-wave bound-free matrix element $r_{fi}^{l\mu\mu}$ of Eq. (4) between the intermediate state and the photoelectron continuum wave function can be written as[17]

$$r_{fi}^{l\mu\mu} = \sum_{l',l_0} \langle \Psi_{kll'}(r) Y_{l'\lambda}(\hat{r}') | r Y_{1\mu} | \Phi_{il_0}(r) Y_{l_0 0}(\hat{r}') \rangle. \tag{5}$$

For a central field potential $l' = l$. The noncentral potential of a molecular ion can give rise to significant $l \neq l'$ terms. Using the symmetry relationship, $r_{fi}^{l\mu\mu} = r_{fi}^{l-\mu-\mu}$, and the properties of the 3-j symbols[25,26] it can be seen by inspection that the last summation in Eq. (4) vanishes unless both $N_t + N_i + N_+ =$ even and $N_t + l =$ odd.[27] This leads to the selection rule,[16]

$$N_+ - N_i + l \equiv \Delta N + l = \text{odd}. \tag{6}$$

An atomiclike picture for which $l' = l$ shows that photoionization via the 8σ Rydberg orbital of the $E^2\Sigma^+(4s\sigma,3d\sigma)$ state or the 9σ orbital of the $H^2\Sigma^+(3d\sigma,4s\sigma)$ state should occur primarily to the odd partial waves of the continuum $(p,f,\ldots)$, i.e., to $l = l_0 \pm 1$. Equation (6) therefore predicts a $\Delta N =$ even rotational propensity rule, similar to the previously predicted,[7-9,17] and experimentally seen[2-4] for the $A^2\Sigma^+(3s\sigma)$ state. Equation (6) does not, however, give the relative intensity nor the number of possible rotational peaks.

The wave functions for the intermediate E and $H^2\Sigma^+$ Rydberg states, with electron configurations $1\sigma^2 2\sigma^2 3\sigma^2 4\sigma^2 5\sigma^2 1\pi^4 8\sigma$ and $1\sigma^2 2\sigma^2 3\sigma^2 4\sigma^2 5\sigma^2 1\pi^4 9\sigma$,[15] respectively, are determined in the improved virtual orbital approximation (IVO)[28] with the extensive Gaussian basis set of Table I. The size and composition of this basis ensures the correct nodal and long-range behavior of the wave functions ($\langle r^2\rangle = 151$ a.u. for the E state and $\langle r^2\rangle = 180$ a.u. for the H state).[29] The IVO method ignores electron correlation effects including Rydberg-valence mixing. The influence of correlation effects on the transition moments have, however, been shown to be minor for such Rydberg states.[2] The close-lying $I^2\Sigma^+$ non-Rydberg state is a possible perturber of the H state. Its dominant configuration is $1\sigma^2 2\sigma^2 3\sigma^2 4\sigma^2 5\sigma^1 1\pi^4 2\pi^2$ which differs from the H-state by a 2-electron excitation and is, hence, not expected to give rise to any significant perturbation. The $H^2\Sigma^+$ state could also be perturbed by the $H'^2\Pi$ state as noted by Huber and Miescher.[23,30,31] This heterogeneous perturbation is disregarded here but could, in principle, be incorporated in the

TABLE I. Gaussian basis set used for the calculations of the Rydberg orbitals of the E and $H\,^2\Sigma^+$ states of NO. (N = nitrogen; O = oxygen; CM = center of mass.)

Contr.	Prim.	Center	Type	Exponent	Coefficient
1	1	N	s	5909.440	0.006 240
1	2	N	s	887.451 0	0.047 669
1	3	N	s	204.749 0	0.231 317
1	4	N	s	59.837 60	0.788 869
2	5	N	s	19.998 10	0.792 912
2	6	N	s	2.686 800	0.323 609
3	7	N	s	7.192 700	1.000 000
4	8	N	s	0.700 000	1.000 000
5	9	N	s	0.213 300	1.000 000
6	10	N	s	0.100 000	1.000 000
7	11	N	p	26.786 00	0.038 244
7	12	N	p	5.956 400	0.243 846
7	13	N	p	1.707 400	0.817 193
8	14	N	p	0.531 400	1.000 000
9	15	N	p	0.165 400	1.000 000
10	16	N	p	0.080 000	1.000 000
11	17	N	d	0.800 000	1.000 000
12	18	O	s	7816.540	0.006 436
12	19	O	s	1175.820	0.048 924
12	20	O	s	273.188 0	0.233 819
12	21	O	s	81.169 60	0.784 798
13	22	O	s	27.183 60	0.803 381
13	23	O	s	3.413 600	0.316 720
14	24	O	s	9.532 200	1.000 000
15	25	O	s	0.939 800	1.000 000
16	26	O	s	0.284 600	1.000 000
17	27	O	s	0.100 000	1.000 000
18	28	O	p	35.183 20	0.040 023
18	29	O	p	7.904 000	0.253 849
18	30	O	p	2.305 100	0.806 842
19	31	O	p	0.717 100	1.000 000
20	32	O	p	0.213 700	1.000 000
21	33	O	p	0.080 000	1.000 000
22	34	O	d	0.800 000	1.000 000
23	35	CM	s	0.025 300	1.000 000
24	36	CM	s	0.011 410	1.000 000
25	37	CM	s	0.005 890	1.000 000
26	38	CM	s	0.003 340	1.000 000
27	39	CM	s	0.002 040	1.000 000
28	40	CM	s	0.001 316	1.000 000
29	41	CM	s	0.000 887	1.000 000
30	42	CM	p	0.044 000	1.000 000
31	43	CM	p	0.019 700	1.000 000
32	44	CM	p	0.010 130	1.000 000
33	45	CM	p	0.005 730	1.000 000
34	46	CM	p	0.003 490	1.000 000
35	47	CM	p	0.002 240	1.000 000
36	48	CM	p	0.001 510	1.000 000
37	49	CM	d	0.082 600	1.000 000
38	50	CM	d	0.036 900	1.000 000
39	51	CM	d	0.018 900	1.000 000
40	52	CM	d	0.006 460	1.000 000

present theoretical framework as previously outlined.[5] The total electronic energy of the NO^+ ion in the basis set of Table I is -128.94407 a.u. at $R = 2.0069$ a.u., in excellent agreement with earlier calculations.[5,15]

The single-center expansion of the molecular orbitals is done around the center-of-mass (CM) of the molecule with a maximum of 20 partial waves in the l_0 expansion. This value ensures an orbital normalization to better than 0.996. In Table II, these expansions and energies are listed for various orbitals. The 8σ and 9σ orbitals are seen to have strongly mixed s and d character leading to unusual quantum defects. This mixing is due to the nonisotropic potential of the ion core. As seen from Table II, the occupied 5σ orbital has significant s and d components and has hence been designated by Jungen[13] as a *precursor core state* for these pairs of ns, $(n-1)d$ Rydberg orbitals, known experimentally to display s and d character. The much studied lower-lying $A\,^2\Sigma^+$ $(3s\sigma)$ state is, hence, the *unusual* ns Rydberg state of NO. Its

TABLE II. Single-center expansion of the NO^+ core and the IVO orbitals about the center-of-mass ($R_e = 2.069$ a.u.).

Orbital	Orbital energy (a.u.)	Partial wave character (%) s	p	d	f	g	h
1σ	−20.639 4	5.181	13.094	16.393	15.773	13.213	10.210
2σ	−15.666 9	5.250	13.253	16.486	15.860	13.182	10.175
3σ	−1.597 59	90.632	1.209	1.003	0.347	3.460	0.211
4σ	−0.785 86	5.007	79.361	5.864	5.857	1.109	1.266
5σ	−0.577 25	48.277	9.047	37.543	1.338	2.770	0.378
1π	−0.589 13	···	82.076	1.731	13.885	0.264	1.639
6σ	−0.129 56	93.981	0.234	5.463	0.060	0.171	0.006
7σ	−0.091 80	0.611	98.794	0.452	0.068	0.003	0.037
8σ	−0.059 87	60.291	0.874	38.743	0.044	0.035	0.001
9σ	−0.053 12	38.217	0.077	61.666	0.004	0.020	0.001

pure "s character" ($>93.9\%$) is due to the lack of a corresponding $(n-1)d$ state.

The photoelectron continuum functions, used in the evaluation of Eq. (6), are obtained using the iterative Schwinger method in the frozen-core-approximation.[32] These photoelectron orbitals are solutions to a one-electron Schrödinger equation containing the nonspherical, nonlocal potential of the molecular core. All matrix elements are evaluated numerically at a single internuclear distance of 2.0069 a.u.[33] The partial wave composition of these resonant orbitals changes little with internuclear distance, unlike the Rydberg states of the diatomic hydrides.[10,12] To assess the possible kinetic energy dependence of these rotational branching ratios in two-color $(2+1')$ REMPI studies of Eq. (1), we have also determined the rotational branching ratios for a range of kinetic energies from 0.05 eV to 6.00 eV.

We have previously shown that the rotational branching ratios and photoelectron angular distributions for REMPI via higher J-levels of the $A\,^2\Sigma^+(3s\sigma)$ state depend on the alignment of the intermediate state.[4,9] To examine this behavior here we have studied the rotational branching ratios and photoelectron angular distributions for the five "possible" types ($\Delta J = 0, \pm 1, \pm 2$) of rotational branches for a 2-photon transition. The open-shell structure of NO and an inability to resolve the individual spin components of the upper $^2\Sigma^+$ states experimentally precludes, however, the existence of "pure" P, Q, and R branches. These rotational branches will be mixed with other rotational transitions with a "mixing ratio" determined by the rotational line strengths B of Eq. (2).[22] We have therefore calculated branching ratios for the pure $O_{11}(23.5)$ and $S_{22}(18.5)$ branches and for the three mixed branches $P_{21}+Q_{11}(21.5)$, $Q_{22}+R_{12}(20.5)$, and $Q_{21}+R_{11}(20.5)$. All these rotational branches go through the N = 21 level of the intermediate state and therefore differ only in the J-level accessed in the intermediate state and hence the alignment created there. The three mixed branches $P_{21}+Q_{11}(21.5)$, $Q_{22}+R_{12}(20.5)$, and $Q_{21}+R_{11}(20.5)$ are the branches with the strongest P, Q, and R branch contributions, respectively.[22] For high-J transitions there are no strong Q-branches, and even the $Q_{22}+R_{12}(20.5)$ branch is strongly dominated by the $R_{12}(20.5)$ branch ($B_{Q_{22}(20.5)}/B_{R_{12}(20.5)} \approx 0.024$). These particular rotational branches are chosen to be representative of the high-J limit, but the results and conclusions presented should also be valid for other J-values.

III. RESULTS

Figure 1 shows the calculated branching ratios for $(2+1)$ REMPI via the $O_{11}(23.5)$, $S_{22}(18.5)$, $P_{21}+Q_{11}(21.5)$, $Q_{22}+R_{12}(20.5)$, and $Q_{21}+R_{11}(20.5)$ branches of the $E\,^2\Sigma^+(4s,3d)$ state of NO. This one-color $(2+1)$ REMPI results in photoelectrons with a kinetic energy of about 2.06 eV.[33] In Fig. 2, we present the similar rotational branches for $(2+1)$ REMPI via the $H\,^2\Sigma^+(3s,4d)$ state of NO, with a photoelectron energy of about 2.39 eV. The rotational branching ratios are all convoluted with a Lorentzian detector function with a full-width-half-maximum (FWHM) value of 4.0 meV, similar to the resolution obtainable in conventional time-of-flight (TOF) photoelectron spectroscopy.[2,4] The propensity for ΔN = even peaks seen here for both the E and the H states with their even l character, is consistent with the selection rule of Eq. (6). The ΔN = odd peaks are less than 5% of the maximum peak and reflect angular momentum coupling in the photoelectron wave function due to the anisotropy of the NO^+ core. The calculated odd ΔN peaks are generally weak compared to those previously seen in REMPI via the $A\,^2\Sigma^+(3s\sigma)$ state of NO.[9] These odd ΔN signals, which have only recently been measured experimentally by Allendorf *et al.* in REMPI via the A state,[4] can be expected to be even more difficult to identify in REMPI via the E and H states. The dependence of branching ratios on rotational branch is also seen to be minor.[4,9]

The rotational branching ratios for REMPI via the A state of NO were dominated by the $\Delta N = 0$ signal, with the $\Delta N = \pm 2$ signals approximately 20% of the $\Delta N = 0$ peak. The calculated branching ratios for REMPI via the $E\,^2\Sigma^+(4s,3d)$ state behave quite differently, with the $\Delta N = \pm 2$ signal the strongest and a $\Delta N = 0$ signal of about 55% of the

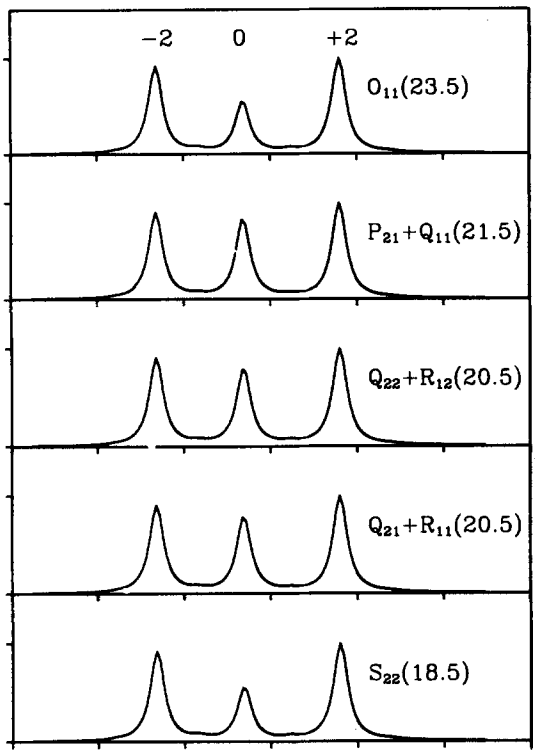

FIG. 1. Ionic rotational branching ratios for (2 + 1) REMPI via the $O_{11}(23.5)$, $P_{21}+Q_{11}(21.5)$, $Q_{22}+R_{12}(20.5)$, $Q_{21}+R_{11}(20.5)$, and $S_{22}(18.5)$ branches of the $E^2\Sigma^+(4s,3d)$ state of NO. The value of $\Delta N \equiv N_+ - N_i$ is indicated above each rotational signal. Photoelectron energy of the $\Delta N = 0$ signal is approximately 2.06 eV. Total length of the abscissa is 120 meV.

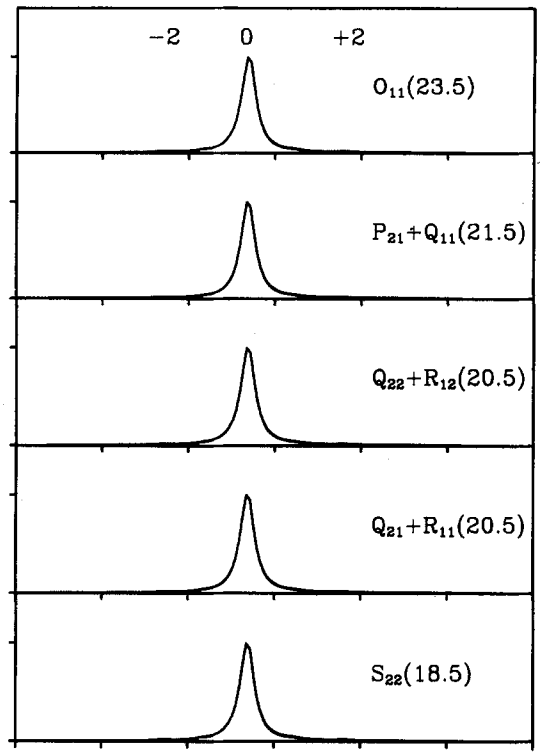

FIG. 2. Ionic rotational branching ratios for (2 + 1) REMPI via the $O_{11}(23.5)$, $P_{21}+Q_{11}(21.5)$, $Q_{22}+R_{12}(20.5)$, $Q_{21}+R_{11}(20.5)$, and $S_{22}(18.5)$ branches of the $H^2\Sigma^+(3d,4s)$ state of NO. The value of $\Delta N \equiv N_+ - N_i$ is indicated above each rotational signal. Photoelectron energy of the $\Delta N = 0$ signal is approximately 2.39 eV. Total length of the abscissa is 120 meV.

$\Delta N = 2$ signal. This dominance of the $\Delta N = \pm 2$ peaks has tentatively been confirmed in preliminary measurements of Leahy *et al.*[20] for REMPI via somewhat lower J branches ($J \sim 13.5$) of the E state. Since these even ΔN signals *only* have contributions from the odd partial waves of the continuum ($l = 1,3,...$) according to Eq. (6), the dominance of the even ΔN peaks indicate that the $r_{fi}^{\mu\mu}$ transition moment of Eq. (5) is largest for the odd partial waves of the continuum. The larger $\Delta N = \pm 2$ signals therefore arise from the higher partial waves in the intermediate Rydberg state, i.e., the d character ($l_0 = 2$) of the E state. Even larger angular momentum transfers could have been expected since the d character of the bound state in an atomic picture leads to both the $l = 1$ and $l = 3$ (p and f) waves of the continuum. The $\Delta N = \pm 4$ signals are, however, found to be almost two orders of magnitude smaller than the $\Delta N = \pm 2$ peaks.

The calculated rotational branching ratios for (2 + 1) REMPI via all the rotational branches of the H state show surprisingly dominant $\Delta N = 0$ signals. The $\Delta N = \pm 2$ peaks are less than 2% of this. The contribution from larger momentum transfer peaks and the odd ΔN peaks is negligible. More than 95% of the total ion signal in the (2 + 1) one-color experiment via the H state of NO is in the $\Delta N = 0$ state. This strong $\Delta N = 0$ propensity for (2 + 1) REMPI via the H state of NO, which offers ion rotational state selection,[11] is caused by the energy dependence of the photoelectron matrix element, $r_{fi}^{\mu\mu}$, of Eq. (5), and its influence on the rotationally resolved transition moment, $\langle f|\mu|i\rangle$, of Eq. (4).[15] Figure 3 shows the partial wave components of $|r_{fi}^{\mu\mu}|$ between the 9σ Rydberg orbital and the $k\sigma$ and $k\pi$ continuum orbitals as a function of kinetic energy. As expected, the transition moments to the p and f waves of the continuum are dominant close to threshold. The $l = 3$ component of the transition moment is seen to be strongly energy dependent with a zero around 2.6 eV in the $k\sigma$ channel and 2.9 eV in the $k\pi$ channel. This minimum in the f-wave transition moment is due to the behavior of the matrix element between the bound Rydberg orbital and the photoelectron continuum orbital, and it is evidence of a molecular Cooper minimum.[34–36] This behavior is present in the $l = l_0 + 1$ partial wave as in Cooper minima via atomic ground states.[34,35] A truly atomic $3d$ orbital does not have a radial node and should therefore not exhibit a Cooper minimum,[35] further demonstrating the molecular nature of the Cooper minimum observed here.

Cooper minima have been studied extensively in atoms[34,35] and in photoionization from molecular ground states,[36] and have recently been identified in optical–optical double resonance spectra in highly excited molecular states of NO,[14] but have not yet been observed in photoionization

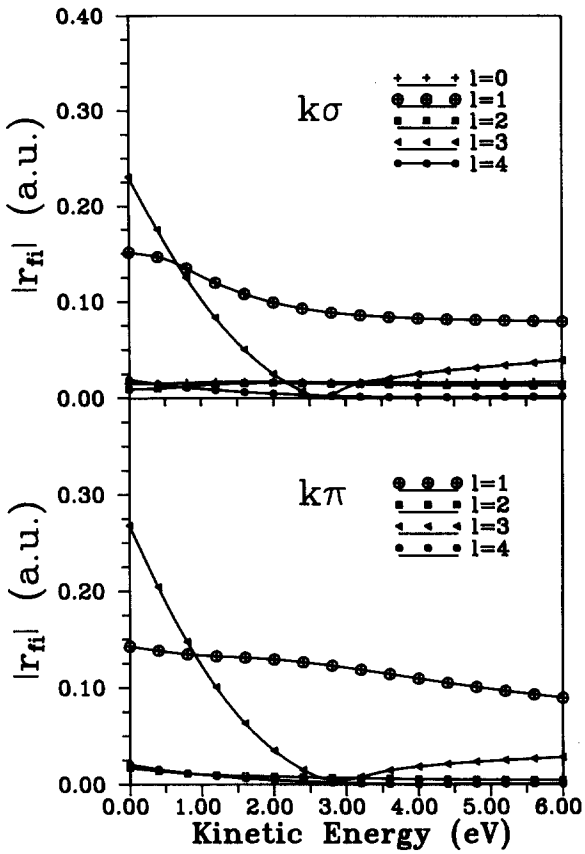

FIG. 3. Partial wave components of the bound-free matrix element, $|r_{fi}^{l\mu\mu}|$, as a function of energy between the 9σ orbital of the $H\,^2\Sigma^+$ state and the $k\sigma$ and $k\pi$ continua, respectively.

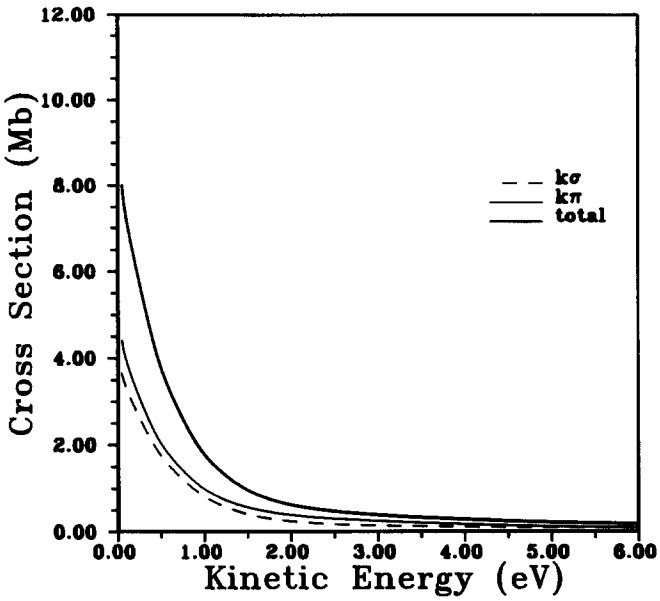

FIG. 4. Total cross section for ionization from the 9σ orbital of the $H\,^2\Sigma^+$ state, rotationally and vibrationally unresolved, as a function of kinetic energy.

via excited molecular states.[37] A Cooper minimum has, however, recently been theoretically identified in the $k\pi$ continuum close to threshold in REMPI via the $D\,^2\Sigma^-$ state of OH.[12] In combination with a rapid orbital evolution this is predicted to lead to strong non-Franck–Condon ion vibrational distributions. The extensive partial wave (l_0's) composition of the molecular orbitals, along with the nonisotropic potentials of their ion core, causes a large number of partial waves (l's) to contribute to the bound-free transition moment $r_{fi}^{l\mu\mu}$. A molecular Cooper minimum most often occurs in a single partial channel, and it is therefore difficult to identify on the basis of its contribution to the total cross section since this will often be dominated by other partial waves.[36] The interference between the partial waves in the photoelectron angular distributions makes the molecular Cooper minimum more readily identified from the measured asymmetry parameter. The significance of a molecular Cooper minimum is enhanced if only a few partial waves contribute to the transition moment, and Cooper minima occur at approximately the same energy in all accessible continuum channels ($k\sigma$,$k\pi$,...).[36] The behavior of the partial wave composition of the photoelectron matrix element around a Cooper minimum also influences the rotational branching ratios. The extent of the influence of a Cooper minimum on the rotational branching ratios depends on the relative magnitude and phases of the partial wave components of the bound-free matrix element. While the influence of the Cooper minimum on the total cross section is negligible, as shown in Fig. 4, its influence on the rotational branching ratios should generally be readily observable also for other molecular systems.

In Fig. 5 and in Table III, we present the calculated rotational branching ratios for $(2+1')$ REMPI via the $O_{11}(23.5)$ branch of the $H\,^2\Sigma^+(3d,4s)$ state of NO. We show only this branch, since the rotational branching ratios are essentially branch-independent. The strong even ΔN propensity rule is evident. The $\Delta N = 2$ peak is strongly energy dependent, being approximately 70% of the $\Delta N = 0$ peak close to threshold, about 2% at the one color energy level (about 2.39 eV) and increasing again to more than 8% at 6.00 eV. This strong energy dependence, as discussed above, is due to the Cooper minimum. A $(2+1')$ experiment with a final kinetic energy of about 500 meV should show strong and easily observable $\Delta N = \pm 2$ peaks. The total cross section is strongly energy dependent, as shown in Fig. 4, and the absolute magnitude of the $\Delta N = 0$ signal at the one-color level is therefore only 15% of its value close to threshold.

The rotational branching ratios for $(2+1')$ REMPI via the $O_{11}(23.5)$ branch of the $E\,^2\Sigma^+(3d,4s)$ state are shown in Fig. 6 and in Table IV. These show only a slight energy dependence. The $\Delta N = \pm 2$ peaks dominate throughout the energy range. Figure 7 shows the partial-wave components of the bound-free matrix element, $|r_{fi}^{l\mu\mu}|$, between the 8σ Rydberg orbital of the $E\,^2\Sigma^+$ state and the $k\sigma$ and $k\pi$ continuum orbitals as a function of photoelectron energy.

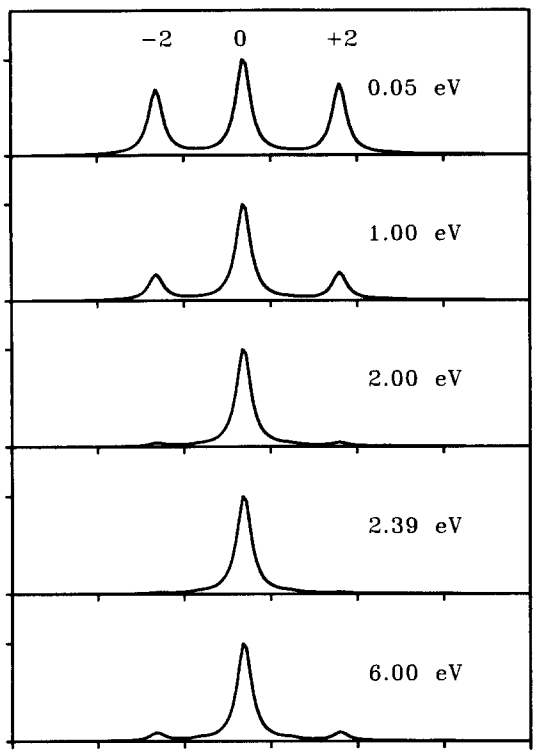

FIG. 5. Ionic rotational branching ratios for $(2+1')$ REMPI via the $O_{11}(23.5)$ branch of the $H\,^2\Sigma^+(3d,4s)$ state as a function of kinetic energy. The value of $\Delta N \equiv N_+ - N_i$ is indicated above each rotational signal. Total length of the abscissa is 120 meV.

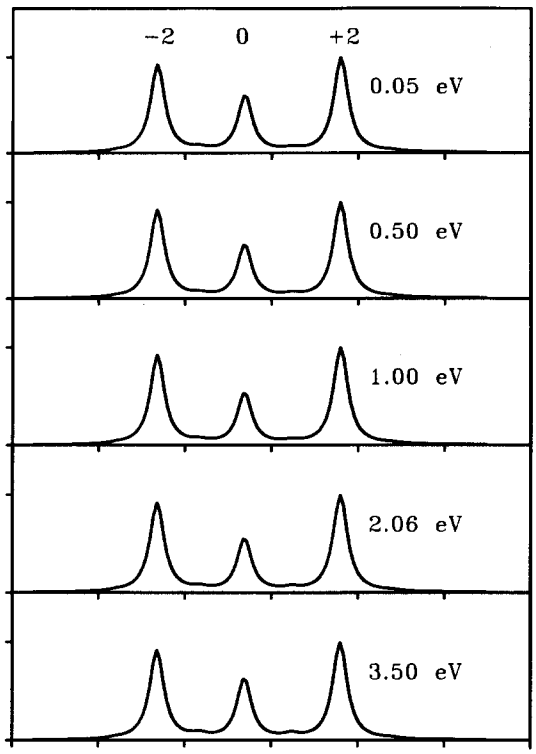

FIG. 6. Ionic rotational branching ratios for $(2+1')$ REMPI via the $O_{11}(23.5)$ branch of the $E\,^2\Sigma^+(3d,4s)$ state as a function of kinetic energy. The value of $\Delta N \equiv N_+ - N_i$ is indicated above each rotational signal. Total length of the abscissa is 120 meV.

The transition moment to the p and f waves of the continuum are dominant throughout the energy range, with no evidence of a Cooper minimum. The differences in the radial function of the 8σ and the 9σ orbitals causes its Cooper minimum to be at a much higher energy (around 15 eV). In Fig. 8, the total cross section for ionization of the 8σ orbital of the E state is seen to be strongly energy dependent, similar to the cross section for the H state.

The photoelectron angular distributions for $(1+1')$ REMPI via the $A\,^2\Sigma^+$ state of NO have been previously shown to depend strongly on the alignment of the intermediate state.[4,9] The calculated photoelectron angular distributions for one color $(2+1)$ REMPI via the five rotational branches, $O_{11}(23.5)$, $P_{21}+Q_{11}(21.5)$, $Q_{22}+R_{12}(20.5)$, $Q_{21}+R_{11}(20.5)$, and $S_{22}(18.5)$, are shown in Figs. 9 and 10 for the E and H states, respectively. The distributions are seen to depend on $|\Delta J|$, in agreement with the result for the $A\,^2\Sigma^+$ state.[9] The mixed $Q_{22}+R_{12}(20.5)$ branch, which is dominated by the R_{12} branch, has angular distributions similar to those of the mixed P and R branches. At this high J value there are only two "types" of angular distributions, for $|\Delta J|=1$ (P and R branches) and for $|\Delta J|=2$ (O and S branches).[22] In Figs. 11 and 12 the dependence of these angular distributions on photoelectron energy are shown for

TABLE III. Calculated angle-integrated rotational branching ratios (normalized to the $\Delta N=0$ signal) as a function of energy for the $O_{11}(23.5)$ branch resulting from $(2+1')$ REMPI via the $H\,^2\Sigma^+(3d,4s)$ state of NO.

		Photoelectron Energy (eV)								
		0.05	0.50	1.00	1.50	2.00	2.39	3.00	3.50	6.00
	−2	0.674	0.452	0.260	0.113	0.035	0.011	0.013	0.022	0.081
	−1	0.005	0.005	0.006	0.009	0.010	0.011	0.011	0.011	0.016
ΔN =	0	≡1.00	≡1.00	≡1.00	≡1.00	≡1.00	≡1.00	≡1.00	≡1.00	≡1.00
	+1	0.005	0.005	0.006	0.009	0.011	0.011	0.011	0.012	0.016
	+2	0.732	0.491	0.282	0.122	0.038	0.011	0.014	0.024	0.088

TABLE IV. Calculated angle-integrated rotational branching ratios (normalized to the $\Delta N = +2$ signal) as a function of energy for the $O_{11}(23.5)$ branch resulting from $(2+1')$ REMPI via the $E\,^2\Sigma^+(4s,3d)$ state of NO.

		Photoelectron Energy (eV)								
		0.05	0.50	1.00	1.50	2.00	2.06	2.50	3.00	3.50
	−2	0.922	0.922	0.922	0.921	0.921	0.921	0.921	0.921	0.920
	−1	0.027	0.026	0.025	0.026	0.028	0.029	0.032	0.036	0.039
ΔN =	0	0.597	0.553	0.530	0.528	0.544	0.546	0.570	0.600	0.627
	+1	0.029	0.028	0.026	0.027	0.029	0.030	0.034	0.038	0.041
	+2	≡1.00	≡1.00	≡1.00	≡1.00	≡1.00	≡1.00	≡1.00	≡1.00	≡1.00

the two states. We show only the result for the $O_{11}(23.5)$ and $P_{21}+Q_{11}(21.5)$ branches since they are representative of all the rotational branches. The rotationally resolved photoelectron angular distributions for the $E\,^2\Sigma^+$ state, particularly for the $\Delta N = 0$ signal, are strongly energy dependent, even though the rotational branching ratios were found to be almost energy independent. The angular distributions for the H state behave similarly with the $\Delta N = \pm 2$ distributions changing dramatically around the Cooper minimum. This behavior will, however, be difficult to observe due to the low value of the $\Delta N = \pm 2$ signals. The rotationally unresolved photoelectron angular distributions are dominated by the strongest rotational transition with a large β_2 value. The β-values of Eq. (3) are listed in Tables V–VIII for the E and H state.

IV. CONCLUSIONS

We have reported rotational branching ratios and photoelectron angular distributions for both one- and two-color $(2+1)$ REMPI via high rotational levels of the $E\,^2\Sigma^+(3d,4s)$ and $H\,^2\Sigma^+(4s,3d)$ Rydberg states of NO. The rotational branching ratios show the expected $\Delta N =$ even propensity rule and depend, in the high J limit, on intermediate

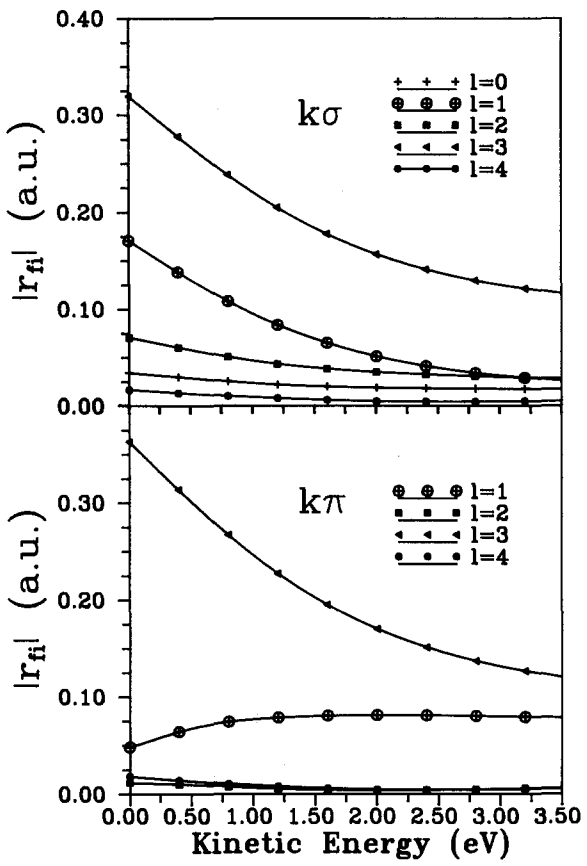

FIG. 7. Absolute value of the partial wave expanded bound-free matrix element, $|r_{fi}^{l\mu\mu}|$, as a function of energy between the 8σ orbital of the $E\,^2\Sigma^+$ state and the $k\sigma$ and $k\pi$ continua, respectively.

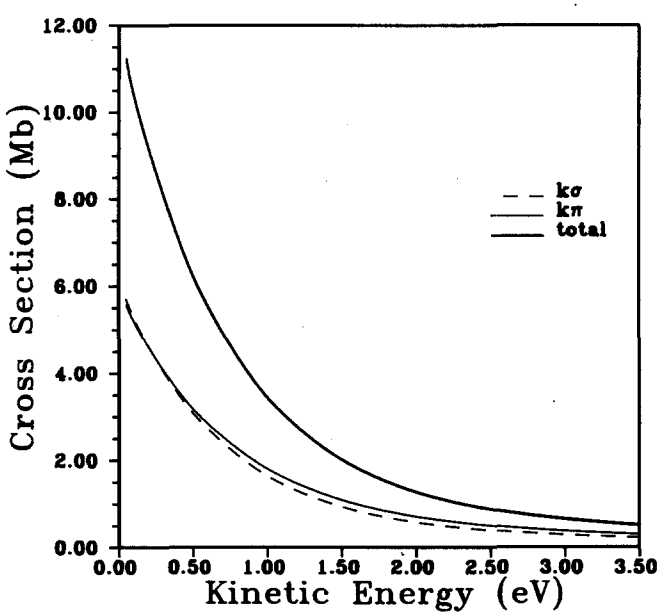

FIG. 8. Total cross section for ionization from the 8σ orbital of the $E\,^2\Sigma^+$ state, rotationally and vibrationally unresolved, as a function of photoelectron energy.

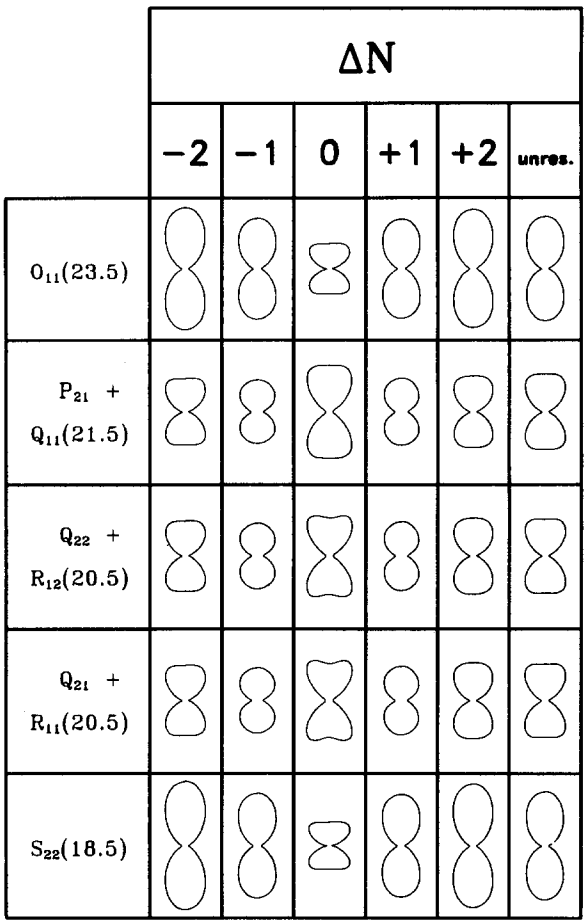

FIG. 9. Photoelectron angular distributions, rotationally resolved and rotationally unresolved, for (2 + 1) REMPI via the $O_{11}(23.5)$, $P_{21}+Q_{11}(21.5)$, $Q_{22}+R_{12}(20.5)$, $Q_{21}+R_{11}(20.5)$, and $S_{22}(18.5)$ branches of the $E^2\Sigma^+(4s,3d)$ state of NO. $\theta = 0°$ is vertical.

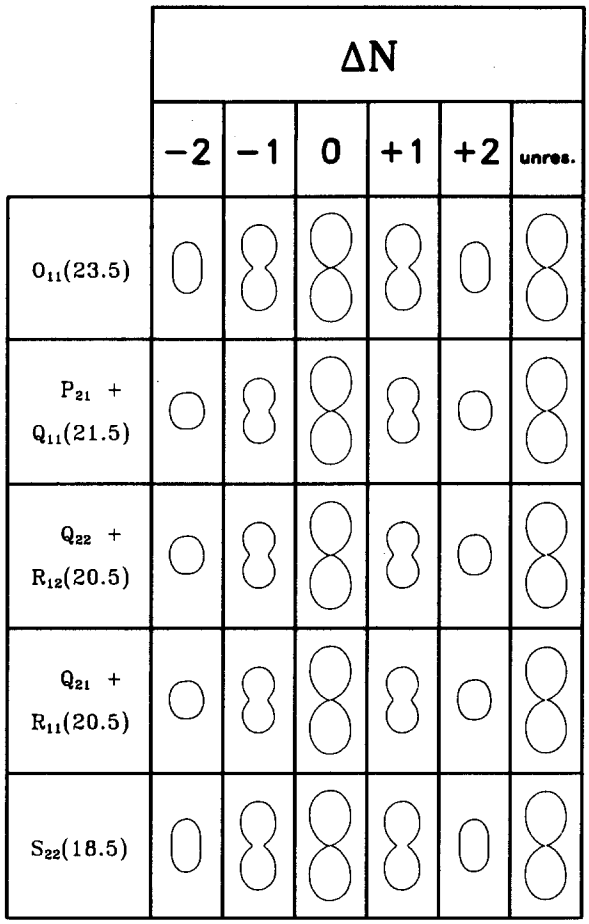

FIG. 10. Photoelectron angular distributions, rotationally resolved and rotationally unresolved, for (2 + 1) REMPI via the $O_{11}(23.5)$, $P_{21}+Q_{11}(21.5)$, $Q_{22}+R_{12}(20.5)$, $Q_{21}+R_{11}(20.5)$, and $S_{22}(18.5)$ branches of the $H^2\Sigma^+(4s,3d)$ state of NO. $\theta = 0°$ is vertical.

TABLE V. Calculated asymmetry parameters (β_{2L}) for the $O_{11}(23.5)$ branch of the $E^2\Sigma^+(3d,4s)$ state of NO as a function of energy, as defined by Eq. (3), with $\beta_0 \equiv 1.000$.

			Kinetic Energy (eV)								
			0.05	0.50	1.00	1.50	2.00	2.06	2.50	3.00	3.50
		β_2	0.92	1.52	1.76	1.88	1.95	1.96	1.99	2.01	2.02
	−2	β_4	0.34	0.41	0.43	0.45	0.45	0.45	0.45	0.46	0.46
		β_6	0.02	0.02	0.02	0.02	0.02	0.02	0.02	0.02	0.02
		β_2	1.59	1.66	1.65	1.66	1.69	1.69	1.72	1.74	1.75
	−1	β_4	0.10	0.13	0.15	0.16	0.16	0.16	0.15	0.13	0.10
		β_6	−0.02	−0.02	−0.02	−0.01	−0.01	−0.01	−0.01	−0.01	−0.02
		β_2	0.83	1.22	1.24	1.16	1.07	1.06	1.00	0.95	0.93
ΔN =	0	β_4	−0.24	−0.17	−0.33	−0.54	−0.75	−0.77	−0.90	−1.00	−1.05
		β_6	0.13	0.14	0.14	0.14	0.14	0.14	0.13	0.12	0.12
		β_2	1.57	1.65	1.64	1.65	1.67	1.68	1.71	1.73	1.73
	+1	β_4	0.06	0.08	0.11	0.12	0.12	0.12	0.11	0.09	0.06
		β_6	−0.02	−0.02	−0.01	−0.01	−0.01	−0.01	−0.01	−0.01	−0.01
		β_2	0.90	1.49	1.73	1.84	1.92	1.92	1.96	1.97	1.98
	+2	β_4	0.31	0.36	0.38	0.39	0.39	0.39	0.40	0.40	0.40
		β_6	0.02	0.02	0.02	0.02	0.02	0.02	0.02	0.02	0.02
		β_2	0.89	1.43	1.62	1.70	1.73	1.73	1.73	1.73	1.72
Rot. unres.		β_4	0.19	0.25	0.24	0.20	0.16	0.16	0.12	0.09	0.06
		β_6	0.04	0.04	0.04	0.04	0.04	0.04	0.04	0.04	0.04

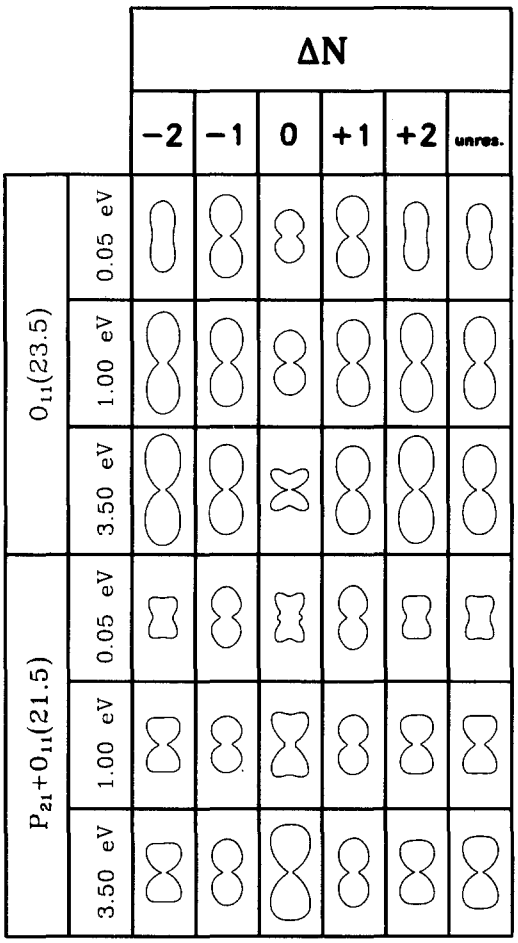

FIG. 11. Photoelectron angular distributions, rotationally resolved and unresolved, for $(2+1')$ REMPI via the $O_{11}(23.5)$ and $P_{21}+Q_{11}(21.5)$ branches of the $E\,^2\Sigma^+$ state for a kinetic energy of 0.05 eV, 1.00 eV, and 3.50 eV, respectively. $\theta = 0°$ is vertical.

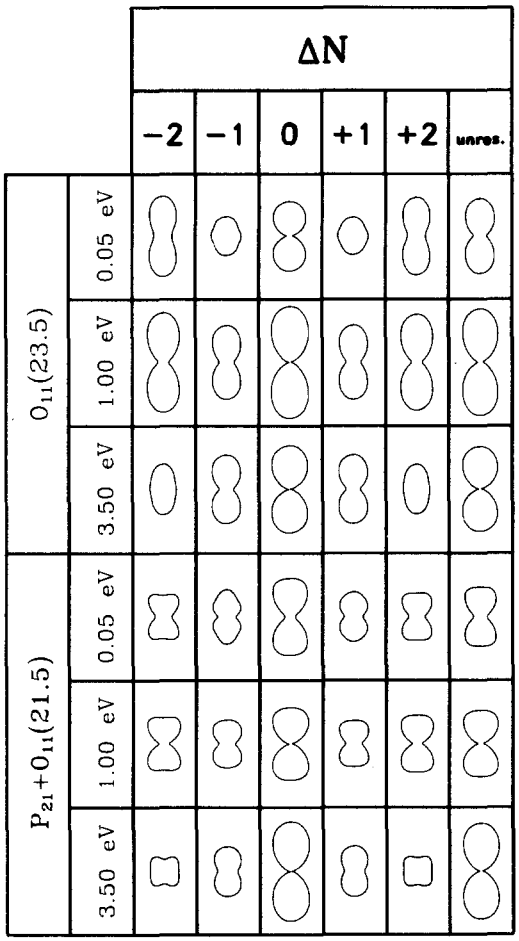

FIG. 12. Photoelectron angular distributions, rotationally resolved and unresolved, for $(2+1')$ REMPI via the $O_{11}(23.5)$ and $P_{21}+Q_{11}(21.5)$ branches of the $H\,^2\Sigma^+$ state for a kinetic energy of 0.05 eV, 1.00 eV, and 3.50 eV, respectively. $\theta = 0°$ is vertical.

TABLE VI. Calculated asymmetry parameters (β_{2L}) for the $P_{21}+Q_{11}(21.5)$ branch of the $E\,^2\Sigma^+(3d,4s)$ state of NO as a function of energy, as defined by Eq. (3), with $\beta_0 \equiv 1.000$.

			Kinetic Energy (eV)								
			0.05	0.50	1.00	1.50	2.00	2.06	2.50	3.00	3.50
		β_2	0.64	1.08	1.26	1.35	1.40	1.40	1.43	1.44	1.44
	−2	β_4	−0.29	−0.38	−0.42	−0.44	−0.46	−0.46	−0.47	−0.48	−0.48
		β_6	−0.13	−0.13	−0.13	−0.13	−0.13	−0.13	−0.13	−0.13	−0.13
		β_2	1.06	1.02	1.00	1.02	1.02	1.02	1.08	1.15	1.21
	−1	β_4	−0.24	−0.28	−0.33	−0.36	−0.35	−0.35	−0.33	−0.28	−0.22
		β_6	0.16	0.14	0.12	0.10	0.09	0.09	0.09	0.09	0.10
		β_2	0.78	1.27	1.57	1.78	1.94	1.96	2.05	2.12	2.16
ΔN =	0	β_4	0.07	−0.15	−0.13	−0.04	0.06	0.07	0.15	0.21	0.25
		β_6	−0.53	−0.54	−0.53	−0.50	−0.47	−0.46	−0.43	−0.40	−0.38
		β_2	1.04	1.09	1.04	1.03	1.05	1.05	1.11	1.18	1.25
	+1	β_4	−0.16	−0.20	−0.25	−0.27	−0.27	−0.27	−0.25	−0.20	−0.15
		β_6	0.13	−0.11	0.09	0.08	0.07	0.07	0.07	0.07	0.08
		β_2	0.66	1.11	1.30	1.39	1.44	1.44	1.47	1.49	1.49
	+2	β_4	−0.24	−0.31	−0.34	−0.36	−0.37	−0.37	−0.38	−0.38	−0.39
		β_6	−0.08	−0.08	−0.08	−0.08	−0.08	−0.08	−0.08	−0.08	−0.08
		β_2	0.68	1.13	1.34	1.47	1.56	1.56	1.62	1.66	1.68
Rot. unres.		β_4	−0.17	−0.29	−0.31	−0.29	−0.27	−0.26	−0.24	−0.21	−0.20
		β_6	−0.22	−0.22	−0.22	−0.21	−0.21	−0.21	−0.20	−0.20	−0.19

TABLE VII. Calculated asymmetry parameters (β_{2L}) for the O_{11} (23.5) branch of the $H\,^2\Sigma^+$ (4s,3d) state of NO as a function of energy, as defined by Eq. (3), with $\beta_0 \equiv 1.000$.

			Kinetic Energy (eV)								
			0.05	0.50	1.00	1.50	2.00	2.39	3.00	3.50	6.00
		β_2	1.15	1.50	1.67	1.72	1.56	0.40	0.12	0.42	0.66
	−2	β_4	0.41	0.43	0.45	0.44	0.37	0.04	0.04	0.17	0.28
		β_6	0.03	0.03	0.03	0.03	0.02	0.00	0.01	0.01	0.02
		β_2	0.19	0.62	1.18	1.45	1.48	1.38	1.27	1.14	0.78
	−1	β_4	0.25	0.16	0.09	0.05	0.03	0.03	0.03	0.03	0.05
		β_6	−0.05	−0.02	0.00	0.00	−0.02	0.00	0.00	0.00	0.00
		β_2	1.44	1.98	2.18	2.20	2.12	2.02	1.95	1.88	1.72
ΔN =	0	β_4	−0.25	0.23	0.35	0.31	0.18	0.03	−0.06	−0.13	−0.29
		β_6	0.06	0.04	0.02	0.01	0.00	0.00	0.00	0.00	0.01
		β_2	0.15	0.60	1.19	1.45	1.49	1.39	1.28	1.15	0.78
	+1	β_4	0.10	0.26	0.16	0.78	0.04	0.02	0.02	0.02	0.02
		β_6	−0.02	−0.02	0.00	0.00	0.00	0.00	0.00	0.00	0.00
		β_2	1.13	1.47	1.64	1.69	1.54	0.39	0.11	0.41	0.65
	+2	β_4	0.35	0.38	0.39	0.39	0.32	0.04	0.04	0.16	0.25
		β_6	0.02	0.02	0.02	0.02	0.01	0.00	0.00	0.01	0.01
		β_2	1.26	1.74	1.99	2.09	2.07	1.96	1.88	1.79	1.53
Rot. unres.		β_4	0.12	0.31	0.37	0.32	0.19	0.03	−0.05	−0.11	−0.20
		β_6	0.04	0.03	0.02	0.01	0.04	0.00	0.00	0.00	0.01

state alignment and not on the particular rotational branch. They were also found to be quite energy independent for the $E\,^2\Sigma^+$ state but strongly dependent for the $H\,^2\Sigma^+$ state. This dependence is caused by a Cooper minimum in the transition moment between the 9σ orbital of the $H\,^2\Sigma^+$ state to the f-wave of the continuum around 2.6 eV for the $k\sigma$ channel and around 2.9 eV for the $k\pi$ channel. The Cooper minima lead to a strong $\Delta N = 0$ propensity rule, with more than 95% of the ions produced in the $\Delta N = 0$ state for a $(2+1)$ one-color experiment via the $H\,^2\Sigma^+$ state. This feature can hence be exploited to obtain ions in specific rotational levels. The photoelectron angular distributions are also seen to be strongly energy dependent for REMPI via both states and display a dramatic change in the $\Delta N = \pm 2$ angular distributions around the Cooper minimum of the H state. This behavior of rotational branching ratios around a Cooper minimum should be quite general, and should be readily observable in REMPI via other molecular Rydberg states. The influence of a Cooper minimum on the rotational branches is, however, expected to be greatest if a Cooper minimum is present in all accessible continuum channels at approximately the same kinetic energy.

TABLE VIII. Calculated asymmetry parameters (β_{2L}) for the $P_{21} + Q_{11}$ (21.5) branch of the $H\,^2\Sigma^+$ (4s,3d) state of NO as a function of energy, as defined by Eq. (3), with $\beta_0 \equiv 1.000$.

			Kinetic Energy (eV)								
			0.05	0.50	1.00	1.50	2.00	2.39	3.00	3.50	6.00
		β_2	0.82	1.07	1.20	1.24	1.13	0.06	−0.30	0.07	0.33
	−2	β_4	−0.32	−0.38	−0.40	−0.39	−0.32	−0.03	−0.08	−0.22	−0.34
		β_6	−0.14	−0.14	−0.14	−0.13	−0.11	−0.02	−0.03	−0.08	−0.12
		β_2	0.64	0.65	0.77	0.92	0.95	0.86	0.77	0.67	0.48
	−1	β_4	−0.32	−0.32	−0.26	−0.16	−0.11	−0.08	−0.08	−0.09	−0.13
		β_6	0.22	0.10	0.02	0.01	0.01	0.01	0.01	0.01	0.01
		β_2	1.61	1.63	1.70	1.80	1.90	1.98	2.02	2.05	2.08
ΔN =	0	β_4	0.10	−0.23	−0.29	−0.22	−0.12	−0.01	0.05	0.10	0.22
		β_6	−0.28	−0.19	−.011	−0.04	−0.01	0.00	0.00	−0.01	−0.03
		β_2	0.65	0.66	0.78	0.93	0.96	0.87	0.78	0.67	0.48
	+1	β_4	−0.18	−0.38	−0.30	−0.18	−0.11	−0.07	−0.07	−0.07	0.10
		β_6	0.09	0.01	−0.03	−0.01	0.00	0.01	0.01	0.01	0.01
		β_2	0.84	1.10	1.23	1.27	1.54	0.11	−0.25	0.10	0.35
	+2	β_4	−0.28	−0.31	−0.32	−0.31	−0.26	−0.03	−0.08	−0.20	−0.29
		β_6	−0.09	−0.09	−0.09	−0.08	−0.07	−0.01	−0.02	−0.05	−0.08
		β_2	1.17	1.37	1.53	1.69	1.83	1.92	1.95	1.95	1.82
Rot. unres.		β_4	−0.13	−0.28	−0.31	−0.25	−0.13	−0.17	0.05	0.09	0.15
		β_6	−0.18	−0.15	−0.11	−0.05	−0.02	−0.01	0.00	−0.01	−0.04

ACKNOWLEDGMENTS

The research was supported by the National Science Foundation (Grant No. CHE-8521391), the Air Force Office of Scientific Research (Contract No. 87-0039), and the Office of Health and Environmental Research of the U.S. Department of Energy (Grant No. DE-FG03-87ER60513). We also made use of resources of the San Diego SuperComputer Center, which is supported by the National Science Foundation. H. R. gratefully acknowledges support from the NATO Science Fellowship Program (Denmark). We would also like to acknowledge helpful discussions with Dr. Richard Zare, Mr. David Leahy, and Dr. James P. Reilly during the preparation of this work.

[1] S. T. Pratt, P. M. Dehmer, and J. L. Dehmer, Chem. Phys. Lett. **105**, 28 (1984).
[2] K. S. Viswanathan, E. Sekreta, E. R. Davidson, and J. P. Reilly, J. Phys. Chem. **90**, 5078 (1986).
[3] M. Sander, L. A. Chewter, K. Müller-Dethlefs, and E. W. Schlag, Phys. Rev. A **36**, 4543 (1987).
[4] S. W. Allendorf, D. J. Leahy, D. C. Jacobs, and R. N. Zare, J. Chem. Phys. **91**, 2216 (1989).
[5] X. Song, E. Sekreta, J. P. Reilly, H. Rudolph, and V. McKoy, J. Chem. Phys. **91**, 6062 (1989).
[6] H. Rudolph, S. N. Dixit, V. McKoy, and W. M. Huo, Chem. Phys. Lett. **137**, 521 (1987).
[7] H. Rudolph, S. N. Dixit, V. McKoy, and W. M. Huo, J. Chem. Phys. **88**, 637 (1988).
[8] H. Rudolph, S. N. Dixit, and V. McKoy, J. Chem. Phys. **90**, 2570 (1989).
[9] H. Rudolph and V. McKoy, J. Chem. Phys. **91**, 1374 (1989).
[10] H. Rudolph, J. A. Stephens, V. McKoy, and M.-T. Lee, J. Chem. Phys. **91**, 1374 (1989).
[11] H. Rudolph and V. McKoy, J. Chem. Phys. **91**, 7995 (1989).
[12] J. A. Stephens and V. McKoy, Phys. Rev. Lett. **62**, 889 (1989).
[13] C. Jungen, J. Chem. Phys. **53**, 4168 (1970).
[14] S. Fredin, D. Gauyacq, M. Horani, C. Jungen, and G. Lefevre, Mol. Phys. **60**, 825 (1987).
[15] K. Kaufmann, C. Nager, and M. Jungen, Chem. Phys. **95**, 385 (1985).
[16] S. N. Dixit and V. McKoy, Chem. Phys. Lett. **128**, 49 (1986).
[17] S. N. Dixit, D. L. Lynch, V. McKoy, and W. M. Huo, Phys. Rev. A **32**, 1267 (1985).
[18] J. C. Miller and R. N. Compton, J. Chem. Phys. **84**, 675 (1986).
[19] Y. Achiba, K. Sato, K. Shobatake, and K. Kimura, J. Chem. Phys. **79**, 5213 (1985).
[20] D. J. Leahy, S. W. Allendorf, and R. N. Zare (private communication).
[21] S. N. Dixit and V. McKoy, J. Chem. Phys. **82**, 3546 (1985).
[22] J. B. Halpern, H. Zacharias, and R. Wallenstein, J. Mol. Spectrosc. **79**, 1 (1980).
[23] H. Lefebvre-Brion and R. W. Field, *Perturbations in the Spectra of Diatomic Molecules* (Academic, Orlando, FL, 1986).
[24] E. Miescher, Can. J. Phys. **49**, 2350 (1971).
[25] A. R. Edwards, *Angular Momentum in Quantum Mechanics*, 2nd ed. (Princeton University, Princeton, NJ, 1974).
[26] I. Kovács, *Rotational Structure in the Spectra of Diatomic Molecules* (Elsevier, New York, 1969).
[27] Note that this condition $N_t + N_i + N_+ =$ even is incorrectly shown as $N_t + N_i + l =$ even just above Eq. 6 of H. Rudolph and V. McKoy, J. Chem. Phys. **91**, 2235 (1989).
[28] W. J. Hunt and W. A. Goddard, III, Chem. Phys. Lett. **128**, 49 (1986).
[29] P. Cremaschi, Chem. Phys. Lett. **83**, 106 (1981).
[30] K. P. Huber and E. Miescher, Helv. Phys. Acta **36**, 257 (1963).
[31] I. Kovács, Helv. Phys. Acta **36**, 699 (1963).
[32] R. R. Lucchese, G. Raseev, and V. McKoy, Phys. Rev. A **25**, 2572 (1982).
[33] K. P. Huber and G. Herzberg, *Constants of Diatomic Molecules* (Van Nostrand Reinhold, New York, 1979).
[34] J. W. Cooper, Phys. Rev. **128**, 681 (1962).
[35] S. T. Manson, Phys. Rev. A **31**, 3698 (1985).
[36] T. A. Carlson, M. O. Krause, W. A. Svenson, P. Gerard, F. A. Grimm, T. A. Whitley, and B. P. Pullen, Z. Phys. D **2**, 309 (1986).
[37] W. A. Chupka, J. Chem. Phys. **87**, 1488 (1987).